Fracture of mass concrete under simulated seismic action

By E. Brühwiler*

Reprinted from

Dam Engineering

VOLUME I ISSUE 3

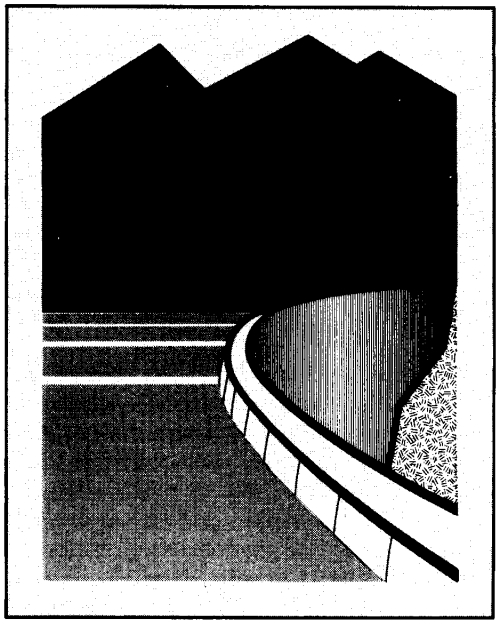

*Research Associate, University of Colorado, Boulder, USA
(Formerly: Swiss Federal Institute of Technology, Lausanne, Switzerland)

Fracture of mass concrete under simulated seismic action

E Brühwiler
Research Associate
University of Colorado
Boulder, USA
(formerly: Swiss Federal Institute of Technology
Lausanne, Switzerland)

SUMMARY

The numerical simulation of concrete dams subjected to earthquake loading requires realistic material laws which take into account material properties as affected by seismic action. Experiments under simulated seismic action were performed to examine the effect of rapid compressive loading on the fracture properties of mass concrete at high tensile deformation rates. Loading histories, representing typical seismic action, were applied to the specimens. Fracture properties have been investigated by two types of tests:

- Uniaxial tensile tests were performed to study the ascending stress against strain curve (up to tensile strength) to describe continuous material under tensile stresses; and,
- wedge splitting tests were conducted to investigate tensile softening properties and cracking of mass concrete.

The test results showed that the effect of high deformation rates and loading histories must be considered in the seismic analysis of dams. The tensile strength and the specific fracture energy showed a high rate sensitivity. Compressive pre-loading led to some damage of the concrete and a significant decrease in the values of fracture properties. A procedure for the development of material laws, based on these results, is proposed.

Introduction

The numerical simulation of concrete dams subjected to earthquakes is a very complex task which has to include aspects such as modelling of crack formation, nonlinear structural behaviour of the dam as a result of cracking, effect of soil-structure and reservoir-structure interaction, effect of construction joints and realistic assessment of the seismic action. For a comprehensive analysis, simple but realistic material laws for the mass concrete are required. Such material laws have to take into consideration conditions which typically occur under seismic action.

Seismic action is characterized by mainly horizontal motions. Irregular vibrations of a frequency of 1 to 15 Hz and maximum ground acceleration of 0.2 to 0.5 g occur. The structure and hence the material is exposed to alternating excitations at high loading rates, expressed by strain rates $\dot{\epsilon}$ of:

$$10^{-4}\mathrm{s}^{-1} < \dot{\epsilon} < 1\mathrm{s}^{-1}$$

Seismic strain rates are much lower than strain rates caused by impact for which $\dot{\epsilon}$ is:

$$1\mathrm{s}^{-1} < \dot{\epsilon} < 100\mathrm{s}^{-1}$$

During an earthquake, several parts of the dam exhibiting compressive stresses under service conditions, may experience tensile stresses. Other parts may be subjected to compression before tensile

stresses form. Since concrete has a relatively low tensile strength, the dam may undergo the formation of structural cracks. Thus, the safety of these large unreinforced concrete structures when subjected to earthquakes is controlled by the tensile behaviour and cracking of concrete.

Efforts have been undertaken to study, both theoretically and empirically, the behaviour of concrete under high loading rates including impact (Mindess & Shah [ed] 1986). A summary of test results and a description of testing methods is provided by Reinhardt (1990). The literature indicates that both tensile and compressive strength of concrete increase with increased strain rate, but the tensile strength is more rate sensitive. Furthermore, theories have been developed to explain the strength increase caused by high loading rates (Curbach 1987, Reinhardt 1986).

Shrinkage resulting from concrete hydration leads to the formation of microscopic cracks in the composite structure. Before concrete is loaded, microcracks exist both in the cement matrix and at the interface boundaries between the matrix and aggregate inclusions. Under loading, these microcracks may grow and join to form continuous cracks. Concrete is likely to undergo damaging processes caused by sustained, static and fatigue loading under compression or tension. Under seismic action, excessive stresses higher than the stresses caused by service loads may occur leading to further material damage and microcracking. To predict the remaining ultimate strength of such structures, the effect of the loading history on the strength and fracture properties of the material must be known. Few investigations on the effect of pre-loading, that is, loading prior to failure of the specimen, on fracture properties of plain concrete are reported in the literature. Recent studies of Hordijk & Reinhardt (1989) and Pons *et al.* (1988) showed that strength and fracture properties are likely to decrease as a result of pre-loading.

The analysis of concrete dams subjected to earthquake is usually performed using the concept of strength of materials. However this concept does not provide a realistic simulation of crack formation and crack propagation in a structure. In this paper, fracture mechanics models are suggested as an alternative. Fracture mechanics provides a more comprehensive description of concrete cracking by considering the inherent nature of the cracking and the stress singularity at the vicinity of a crack. Yet, there is a lack in knowlwedge of fracture properties as influenced by seismic action.

This paper reports on fracture experiments conducted under simulated seismic action. Mass concrete specimens are examined to study the effect of rapid compressive loading on fracture properties of mass concrete at high deformation rates. Fracture properties are discussed in view of their engineering application to modelling of crack formation in concrete dams subjected to seismic action.

1 Modelling of crack formation under seismic action

Until the late seventies, the only concept for crack growth was based on a strength criterion in which the crack was assumed to propagate whenever the computed tensile stresses exceeded the tensile strength of the material. However, the strength criterion does not account for the stress singularity that exists at the crack tip, and, the analysis was found to be dependent on the size of the finite element mesh (Bažant & Cedolin 1979). As the mesh size is reduced, the analysis is more likely to capture the stress singularity at the crack tip, and higher stresses are computed. Hence, any result could be obtained by simply modifying the element size, demonstrating the futility of the strength approach. Additionally, the strength approach does not account for the structural size effect inherent in dams. Brittle structures such as unreinforced concrete masses show smaller strength with larger structural size. This phenomena, called structural size effect, was observed first by Galileo in the 17th Century (Galileo, G. 1638).

Crack formation in dams and the subsequent nonlinear structural behaviour are more realistically analysed using fracture mechanics approaches. Fracture mechanics takes into account the stress singularity at the crack tip and the inherent nature of concrete cracking. The static response of dams based on a fracture mechanics model has been addressed by many authors (Saouma *et al.* 1990), but very few researchers have investigated the response of dams under seismic action using a fracture mechanics model. While numerous fracture mechanics models have been presented for

concrete (Elfgren (ed.) 1989), two major groups of models, linear elastic and fracture energy models, are of relevance to the analysis of concrete dams.

Fracture energy models are for the most part attributed to Hillerborg *et al.* (1976) for the discrete crack approach in their Fictitious Crack Model (see Section 2) and Bažant & Oh (1983) for the smeared crack approach. The fracture parameters of the fracture energy models are the specific fracture energy, G_F, the tensile strength, f_t, and the softening diagram (describing the relationship between the stress and the width of the fracture process zone). A discrete crack model incorporating the fictitious crack model of Hillerborg has been used for dynamic analysis of a gravity dam by Feltrin *et al.* (1990).

Linear elastic fracture models are a direct adaptation of classical Linear Elastic Fracture Mechanics (LEFM) with the fracture toughness, K_{Ic}, as the material parameter describing fracture resistance of concrete. LEFM has been used in the numerical simulation of gravity dams during an earthquake. Chapuis *et al.* (1985) developed a finite element approach based on LEFM combined with a discrete crack model to analyse crack propagation of Pine Flat dam. Further developments of this approach have been made by Droz (1987) who used crack propagation based on LEFM but combined with a smeared crack model to prevent remeshing. Ayari & Saouma (1990) presented a LEFM approach for the structural response of the dam under seismic action. This approach is based on a discrete crack model and accounts for crack contact/impact of a closing crack (Ayari & Saouma 1989) and crack growth under seismic action.

In modified linear elastic fracture models, classical concepts of LEFM are maintained by using an 'effective' crack which is longer than the true crack but shorter than the true crack plus the fracture process zone (FPZ, see Figure 1c). This is required because classical LEFM models do not account for the FPZ presence. The critical stress intensity factor, or fracture toughness, K_{Ic}, is used in the LEFM structural analysis. For the determination of objective K_{Ic}-values using laboratory specimens, LEFM with an effective crack concept is applied (Saouma *et al.* 1989). The fracture toughness can also be estimated using the relationship between K_{Ic} and G_F from classical LEFM as derived by Irwin (1957) for plane stress conditions:

$$K_{Ic} = \sqrt{G_F \cdot E} \tag{1}$$

where E is the Young's modulus.

2 Softening behaviour of concrete

Fracture properties evaluated from test data must be interpreted in close conjunction with the fracture model considered. Consequently, before discussing fracture properties of mass concrete under seismic action, the inherent nature of concrete cracking and the fracture models considered in this paper must be defined.

A typical stress against strain (elongation) relationship for a mass concrete from a uniaxial tension test is shown in Figure 1a. The experiment was performed under deformation control which enabled the descending post-peak branch to be tracked. At the beginning of the experiment, a linear relationship between stress and elongation was obtained for up to 60 % of the maximum stress. Then, microcracks within the specimen were extended which is indicated by the nonlinearity in the stress against elongation curve up to tensile strength f_t as shown in Figure 1b.

In the post-peak regime, more microcracks are developed in the weakest cross section of the specimen. As mentioned above this localized zone with extensive microcracking is called the fracture process zone (FPZ). The microcracks away from the FPZ are unloaded elastically, while the FPZ shows a continual decrease of its tensile carrying capacity from a peak stress of f_t to 0, together with an increase in deformation. More and more microcracks are formed until finally they coalesce into a macrocrack, while the specimen still can take a substantial load. Thus, a visible crack is no proof that the stress has fallen to zero. Another consequence of microcracking is that the load carrying capacity of the tensile specimen is not yet exhausted when the tensile strength is reached. Fracture energy

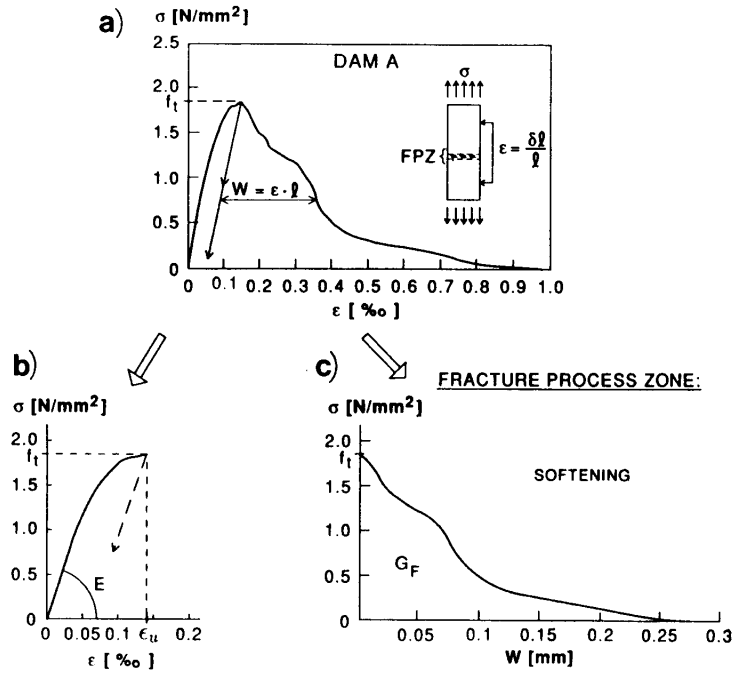

Figure 1. (a) Typical stress against elongation curve of a mass concrete from a tension test, with a division of the deformation properties into: (b) σ against ϵ ($\epsilon = 1\ ‰ = 10^{-3}$), and (c) σ against w curve, where w is the additional deformation caused by the formation of the FPZ.

needs to be added to completely fracture the specimen. In the post-peak regime, all fracture energy is consumed in the FPZ. This material behaviour shown in Figure 1c is called tensile softening.

As a consequence of the inherent nature of concrete cracking, the overall tensile stress against strain relationship is separated into two parts, and the tensile behaviour of concrete is modelled by two constitutive relationships:

1. a stress-strain relationship up to tensile strength, f_t, for the continuous material (Figure 1b); and,
2. a softening law, that is, the relationship between tensile stress σ and width w of the FPZ, to describe fracture of concrete (Figure 1c).

The well-known stress against strain relationship from the strength approach is thus supplemented with fracture mechanics by the use of the softening law for a more comprehensive description of crack formation. The capability of concrete to consume additional energy before complete failure may play an important role with regard to seismic action where the dam structure has to absorb energy arising from ground motion.

Concrete cracking with tensile softening is realistically modelled by the Fictitious Crack Model (Hillerborg *et al.* 1976, Hillerborg 1983). The stress distribution in the vicinity of a crack in a section

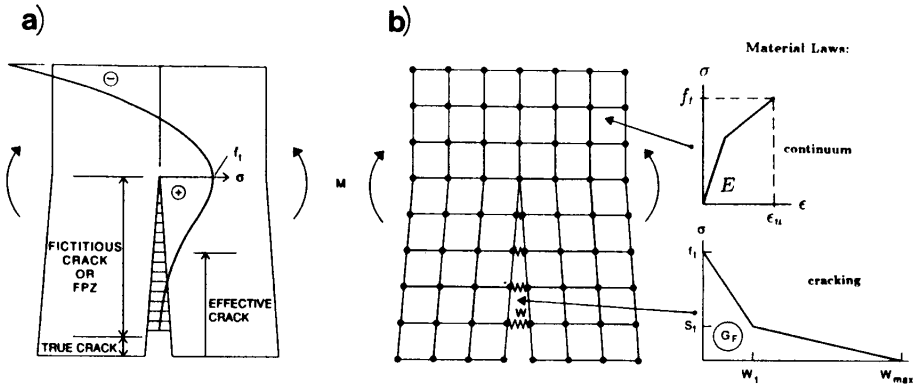

Figure 2. Fictitious Crack Model: (a) stress distribution in the vicinity of a crack in a softening material along the fracture ligament, and (b) Fictitious crack model applied in the analysis of a member subjected to a bending moment M.

subjected to a bending moment is shown schematically in Figure 2a. The fracture process zone is described by a fictitious crack which is located in front of a 'true' (traction-free) crack where the material is completely separated. Along the fictitious crack, the stresses decrease with increasing width of the FPZ, becoming zero at the true crack. No stress is assumed to be larger than the tensile strength. The stress at the tip of the fictitious crack is equal to the tensile strength, and each increase of deformation results in the growth of both fictitious and true cracks. Outside the FPZ, the material is continuous and is described by the stress-strain relationship. The concept of the Fictitious Crack Model is applied using finite element methods (Figure 2b). The propagation of a fictitious crack is simulated by separating elements and introducing nodal forces as functions of both the distance between two nodes (that is, the width of the fictitious crack) and the softening relationship.

The fracture parameters of fracture energy models include the specific fracture energy G_F, the tensile strength f_t and the softening law. G_F is the energy necessary to create a unit crack surface, and is determined by means of stable fracture tests where the energy to fracture a specimen into halves is measured. G_F is numerically equal to the area under the softening diagram. The softening relationship approximated as a bilinear descending branch, is evaluated by means of numerical methods (see Section 4.34). The characteristic length l_{ch} is a material property which is introduced as a measure of the length of the FPZ in a structure:

$$l_{ch} = \frac{G_F \cdot E}{f_t^2} \tag{2}$$

The larger the l_{ch} of the concrete, the longer the fracture process zone in a given structure.

3 Fracture properties of mass concrete at a quasi-static deformation rate

Mass concrete used for the construction of dams and structural concrete differ mainly in the nature and in the size of the aggregates as well as in the cement content. Also, aggregates of mass concrete have their origin in the neighbourhood of the dam. Consequently, extrapolation from structural

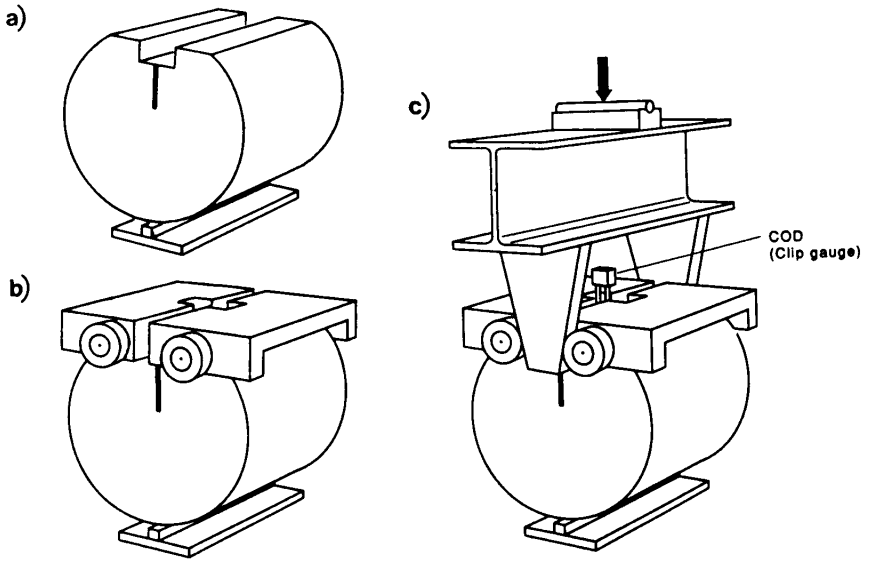

Figure 3. Principle of the wedge splitting test: (a) cylindrical specimen on a linear support; (b) placing of two loading devices with roller bearings; and, (c) the wedges are pressed between roller bearings in order to split the specimen into halves.

concrete to mass concrete cannot be made directly, and, experiments using core material from a specific dam must be conducted for evaluation of reliable material properties.

Wedge splitting tests (Brühwiler 1988, Brühwiler & Wittmann 1990, see Figure 3) were performed to determine the specific fracture energy G_F of mass concrete. The principle of this fracture experiment consists in splitting a notched specimen by means of wedges pressed between roller bearings which are placed on the top of the specimen. Wedge splitting specimens have a large fracture area compared to the specimen weight. This testing method is suitable for testing of mass concrete as drilled cores can easily be used as specimens.

Cylindrical wedge splitting specimens drilled from three existing dams were examined (Brühwiler 1988) from which bilinear softening relationships (Figure 6) were evaluated using the numerical method described in Section 4.34. All tests were performed under deformation control to enable stable fracture of the specimen and the monitoring of the descending branch of the force against deformation curve. A quasi-static deformation rate, or crack opening displacement (COD) rate, was chosen so that the maximum force occurred after 60 to 100 seconds. The specific fracture energy G_F is obtained from the area under the overall splitting force F_s against deformation (COD) curve (Figure 10) divided by the fracture ligament area (ligament length × specimen thickness).

The experimentally determined G_F value depends on the length of the fracture ligament for small specimen sizes, but becomes constant for large specimens with ligament lengths longer than 300 to 400 mm (Brühwiler 1988, Saouma *et al.* 1989). Consequently, the G_F values which were all determined on specimens with ligament lengths smaller than 300 mm were corrected to obtain objective values. According to experimental results, G_F was increased by 20 N/m per 100 mm of additional ligament length up to 300 mm ligament length. Mean values of at least four experiments per type of mass concrete are summarized in Table 1 and compared to typical values of structural

Table 1. Fracture properties (mean values) of mass concrete.

Concrete type	d_a [mm]	f_t [N/mm^2]	E [N/mm^2]	G_F [N/m]	$l_{ch} = \frac{EG_F}{f_t^2}$ [mm]	w_{max} [mm]	K_{Ic} [MN/m$^{3/2}$]
Arch dam A	80	2.4	36 000	230	1 440	0.25	2.9
Arch dam B	120	2.3	27 000	310	1 580	0.30	2.9
Arch dam C	120	2.0	29 000	270	1 960	0.37	2.8
Structural concrete	32	3.4	36 000	140	440	0.16	2.2

d_a = maximum aggregate size

concrete. K_{Ic} was calculated using Eq. 1, and w_{max} was obtained using the method described in Section 4.34. E and f_t were determined in uniaxial compression and tension tests respectively.

The G_F values of the tested mass concretes are significantly larger than the same values of structural concrete. Since the tensile strength f_t and the modulus of elasticity E of mass concrete are smaller than those obtained for structural concrete, the characteristic length l_{ch} is up to 4.5 times longer than for structural concrete. As a consequence, the fracture process zone in dams may be large, and fracture energy models, which account for the presence of FPZ, should be applied for dam structures like arch dams, buttress dams and the crest section of gravity dams (Brühwiler 1988, Brühwiler *et al.* 1989).

The bilinear softening diagrams revealed large crack width values for mass concrete. The maximum width w_{max} of FPZ of mass concrete was about 2 times larger than for structural concrete. The fracture toughness of the mass concretes is about 28 % larger than K_{Ic} of structural concrete (as shown in Table 1).

The fracture surface of the mass concrete specimens was characterized by a relatively large number of aggregate failures as opposed to structural concrete with a great number of failures of the bond between aggregates and cement matrix. This may be explained by additional energy dissipation caused by the multiple crack formation which is more likely to occur in concretes with large aggregates. Also, a lot of energy is probably needed to break aggregates like gneiss, which has a laminar texture, and granite. The high G_F value of mass concrete is thus the result of both the aggregate size and the material properties of the aggregates used for the mass concrete.

4 Experiments under simulated seismic action

Two different kinds of experiments were conducted.

- Uniaxial tensile tests were performed to study the ascending branch of the tensile stress against strain curve of the mass concrete (Figure 1b) as influenced by rapid compressive pre-loadings and high strain rates. A more detailed description of these experiments is provided in Brühwiler (1987).

- Wedge splitting tests were performed to examine the effect of compressive pre-loadings and high deformation rates on the descending softening branch of the complete tensile stress against strain curve of the mass concrete (Figure 1c).

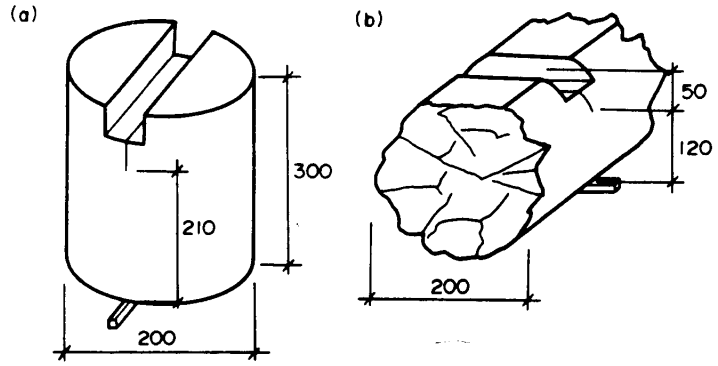

Figure 4. Wedge Splitting Tests: dimensions (in mm) of the specimens used to investigate the effect of (a) deformation rate; and, (b) pre-loading on fracture properties.

4.1 Test specimens

Cylindrical specimens having a diameter of 200 mm and a height of 600 mm, were drilled from blocks which have been poured on the building site of an arch dam in the Swiss Alps. The mass concrete (dam A in Table 1) with a cement content of 250 kg/m^3 and a water-cement ratio of 0.5 was manufactured of mainly crushed (subangular) aggregates with a maximum aggregate size (d_a) of 80 mm. These aggregates consisted of limestone and metamorphic rocks such as granite, gneiss, mica shist and quartz. The strength of the mass concrete was determined on cylinders with a diameter of 200 mm and a height of 600 mm. A compressive strength f_c = 39 N/mm^2, tensile strength f_t = 2.4 N/mm^2 and Young's modulus E = 36 000 N/mm^2 (both in tension and in compression) were determined at an age of two years.

Cylindrical specimens having a diameter of 200 mm and a height of 600 mm were used for the uniaxial tensile tests (Figure 5a). Two different kinds of wedge splitting specimens were examined:

- The effect of deformation rate on fracture properties was studied using cylindrical specimens shown in Figure 4a.
- Fragments of cylinders previously tested and pre-loaded in the tensile test series, were used to investigate the effect of compressive pre-loading on fracture properties at a quasi-static deformation rate (Figure 4b). As with the uniaxial tensile tests, the fracture surface of these wedge splitting specimens was perpendicular to the axis of the cylinder.

The dimensions of the cylindrical specimens were relatively small compared to the maximum aggregate size, that is, smaller than three times the maximum aggregate size. Nevertheless, test results showed relatively low scatter. This may be explained by the fracture behaviour of the examined mass concrete, which was mainly characterized by aggregate failures.

4.2 Description of the experiments

4.21 Uniaxial tensile tests

Uniaxial tensile tests on mass concrete cylinders (Figure 5a) were controlled by means of deformation (strain). To examine the effect of rapid compressive pre-loading on the tensile behaviour at high

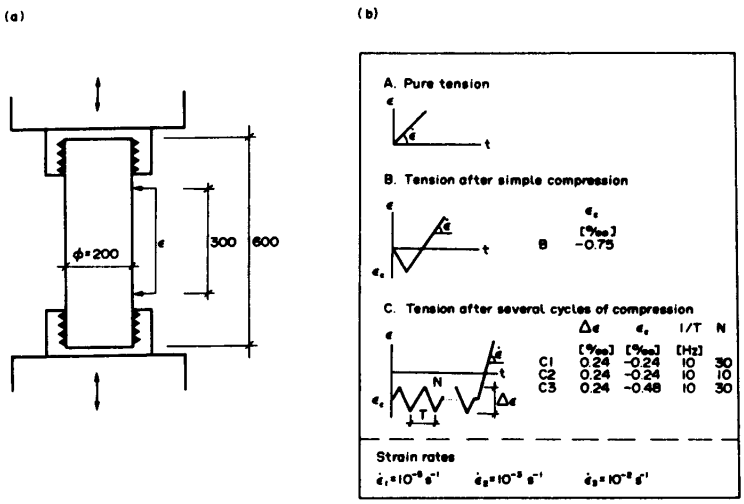

Figure 5. Uniaxial tensile tests: (a) test method, and (b) strain histories.

strain rates, the following strain histories (representing typical seismic action) were applied to the specimens (Figure 5b):

- **A. Direct or pure tension:** tensile deformation up to failure at different strain rates. At the highest strain rate of $\dot{\epsilon} = 10^{-2}s^{-1}$, the time from 0 stress to f_t was about 0.01 seconds.
- **B. Tension after simple compression:** single compressive deformation to a predetermined level and subsequent tensile deformation up to failure at different strain rates. The maximum compressive strain corresponded to about 72 % of the quasi-static compressive strength f_c.
- **C. Tension after several cycles of compression:** repeated compressive cycles at constant amplitude with subsequent tension up to failure at different strain rates. The maximum compressive strain corresponded to about 38 % in series C1 & C2 and 57 % in series C3 of the compressive strength.

Three different tensile strain rates $\dot{\epsilon}$ for the final tension were chosen: $10^{-5}s^{-1}$ corresponding to quasi-static strain rate, $10^{-3}s^{-1}$ and $10^{-2}s^{-1}$ which are in the range of strain rates occurring during an earthquake. In a deformation controlled tensile test, the overall load against deformation curve with a descending branch can generally be recorded. This complete curve was monitored at the quasi-static strain rate (Figure 1a). However, at high deformation rates, the experiments could not be controlled after the peak had been reached, because of insufficient piston velocity of the testing machine. Consequently, sudden failure of the specimen occurred at maximum stress.

4.22 Wedge splitting tests

The Wedge splitting tests on the same mass concrete were all performed under deformation or crack opening displacement (COD) control. In the first test series, the effect of deformation rate, or COD rate, on G_F, the softening diagram and K_{Ic} was examined using the specimen shown in Figure 4a. For

the highest deformation rate of 10 000 times the quasi-static rate, a strain rate of $\dot{\epsilon}$ of $5 \cdot 10^{-2} s^{-1}$ at the notch tip was estimated. The applied deformation rates were thus in the range of seismic strain rates. In the second series, the effect of compressive pre-loading on fracture properties was investigated using the specimen shown in Figure 4b. All experiments were performed at the quasi-static deformation rate.

4.3 Normalization and evaluation of results

4.31 Normalization

Four tests have been performed for each test parameter, that is, the deformation rate and the loading history (as presented in Section 4.21). In this paper, only mean values and mean curves are shown, and, relationships between fracture properties and test parameters as evaluated by a least squares fit are discussed. The main objective of the experiments was to capture the effect of deformation rate and compressive pre-loading on the fracture properties. Absolute values are only of minor importance; consequently, all results were normalized. The quasi-static properties of the mass concrete which was not pre-loaded served as reference values for the normalization.

Assuming that the observed effects of rate and pre-loading are also valid for other mass concretes, a more general use of the test results is achieved by the normalization. Absolute values for other mass concrete properties are then obtained using the normalized relationhips and the reference value for the concrete in question. Hence, the reference value should be a value which can be determined by means of standardized tests, that is, the quasi-static properties of concrete which has not been pre-loaded.

4.32 Description of rate sensitivity

In this paper, the rate sensitivity of fracture properties is expressed by a power law:

$$S_r = S_0 \cdot (\dot{v})^p \tag{3}$$

where S_r is the rate sensitive fracture property; S_0 is any fracture property determined at quasi-static rates; $\dot{v}$ is the deformation rate; and, p is an exponent determined from the test results by a least squares fit. In the uniaxial tensile experiments, deformation is expressed in terms of strain ϵ. A relative deformation rate $\dot{v}_r$ and strain rate $\dot{\epsilon}_r$ is introduced where the relative rate is the ratio between actual and quasi-static rate. A relative rate of $\dot{v}_r = 1$ and $\dot{\epsilon}_r = 1$ describes the same rate.

The use of a power law for the description of rate sensitivity is based on a study by Mihashi & Wittmann (1980) who have predicted a power law for the rate sensitivity of strength by means of a stochastic approach. However, this power law is valid only for strain rates $\dot{\epsilon}$ up to about 1 s^{-1} which corresponds to the upper level of strain rates occurring during earthquakes. On a log-log scale, strength increases linearly with deformation rate according to Eq. 3, and an exact knowledge of the rate of deformation is thus not always required.

In load-controlled experiments, a stress rate $\dot{\sigma}$ is applied to the specimen. Many test results in the literature are expressed as a function of $\dot{\sigma}$. Stress rate may approximately be converted to strain rate by using Hooke's law: $\dot{\epsilon} = \frac{\dot{\sigma}}{E}$.

Inertia forces occurring when the specimen is accelerated from zero to the highest applied deformation rate, were analysed and found to be two orders of magnitude smaller than the total monitored force in the experiments with the highest deformation rate. When the specimen is subjected to a constant deformation rate, acceleration and, hence, inertia forces are zero. As a consequence, inertia effects were not considered in the evaluation of the tests.

4.33 Quantification of pre-loading

The main physical mechanism of concrete fracture is damage resulting from the nucleation and growth of microcracks. Microcracking can be considered as an irreversible damage of the composite structure of concrete with subsequent degradation of material properties. This interpretation of concrete fracture led to the development of damage models (Lorrain & Loland 1986). In the scalar damage model of Mazars (1981), a scalar value D_s is introduced to describe the accumulated damage:

$$S_d = S_0 \cdot (1 - D_s) \tag{4}$$

where S_d is the fracture property affected by damage. S_0 is any fracture property of the undamaged concrete, and D_s is the damage coefficient of the corresponding material property. D_s varies between the value of 0 for undamaged concrete and 1 which means fracture of the material. Accordingly, the intensity of compressive pre-loading histories was quantified in two ways in order to assess a damage coefficient:

1. The energy dissipated during compressive pre-loading was determined from the area under the compressive stress against strain diagram including the energy dissipated during loading cycles. This dissipated energy was then normalized with respect to the energy as determined under the stress against strain curve up to compressive strength in the quasi-static compression test. This damage coefficient is designated $D_s(energy)$ (Figure 12a).

2. The maximum applied compressive strain level $\epsilon_{c,max}$ during pre-loading was normalized with respect to the strain value ϵ_{cc} (= 1.55 °/oo) obtained at maximum compressive stress in the quasi-static compression test. This damage coefficient is designated $D_s(strain)$ (Figure 12b).

4.34 Evaluation of the softening diagram

The most direct way to determine the tensile softening diagram of concrete is the uniaxial tensile test (Figure 1) which is difficult to carry out, especially at high deformation rates. To overcome this difficulty, technically less difficult fracture experiments such as the three point bending test and the wedge splitting test are performed, and simplified models representing the real softening behaviour are evaluated. Roelfstra & Wittmann (1986) showed by means of a finite element analysis based on the fictitious crack model how a bilinear softening diagram can be determined from the experimentally obtained force against deformation curves by a data fit. The wedge splitting test is simulated numerically and then the calculated force against deformation curve is compared to the experimental curve. The parameters of the input softening diagrams are optimized until good agreement between the calculated and experimental curves is obtained. The softening diagram leading to this good agreement is considered to be the tensile softening diagram of the tested concrete.

The parameters of the bilinear softening diagram are, according to Figure 6a: the tensile strength, f_t; the stress, s_1, at the break point; the width of the fictitious crack, w_1, at the break point; and, the maximum fictitious crack width, w_{max}. The specific fracture energy G_F is represented by the area under the softening diagram. For reasons of comparisons, the numerically evaluated softening diagrams are normalized according to Figure 6b where:

$$C_i = \frac{w_i}{\frac{G_F}{f_t}} \tag{5}$$

$$A_N = 1 = (C_1 + \frac{C_{max}}{\frac{f_t}{s_1}}) \cdot 0.5 \tag{6}$$

In the normalized representation, characteristics regarding a test parameter may eventually be captured. If such a characteristic is found, the real softening diagram for different types of concretes can be determined without numerical analysis. It is obtained by a back-transformation from the

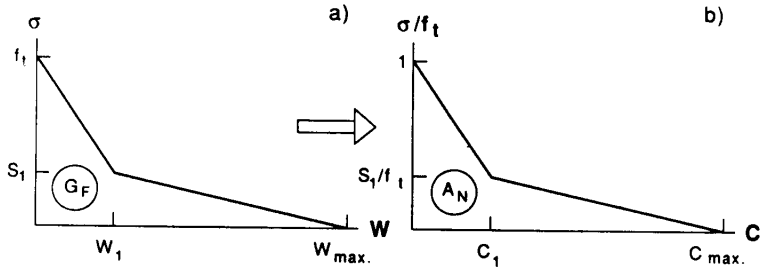

Figure 6. Bilinear softening diagrams (a) as used in the numerical analysis, and (b) in the normalized presentation.

normalized softening law using the corresponding f_t and G_F values as determined by independent tests.

4.4 Results from uniaxial tensile tests

4.41 Direct tension tests (Series A)

The tensile stress against strain mean curves of the tested mass concrete at various strain rates and the relationship between strain rate and f_t are plotted in Figure 7. The following power laws have been determined (Figure 7b and 11):

$$f_t = f_{t,0} \cdot (\dot{\epsilon}_r)^{0.081} \tag{7}$$

$$E = E_0 \cdot (\dot{\epsilon}_r)^{0.020} \tag{8}$$

where $\dot{\epsilon}_r$ is the relative strain rate, that is, the ratio between actual and quasi-static strain rate. The results show that both the tensile strength and the Young's modulus increase with increasing strain rate. At $\dot{\epsilon} = 10^{-2}$ s^{-1}, f_t and E increase by 70 and 16 %, respectively, when compared to the values obtained at the quasi-static strain rate. Comparison with the rate sensitivity given in the literature for structural concrete indicates that mass concrete is more rate sensitive than structural concrete for which an exponent p in the range of 0.045 to 0.065 was determined. The rate sensitivity of the mass concrete with the lower strength is larger than those of structural concrete with the higher strength. Hence, the exponent p is a parameter which depends on the concrete quality. This result is supported by the literature (Reinhardt 1990).

Ultimate strain ϵ_u is the strain at tensile strength. The expression ultimate strain stems from 'unstable' experiments where failure occurs at maximum stress. As shown in Section 2, specimen deformation increases with decreasing stress in the post-peak regime of deformation controlled, stable tests. Nevertheless, ultimate strain is still useful because it determines the transition from a continuous material to macroscopic crack formation. Figure 7a shows that the ultimate strain ϵ_u is not affected by strain rate. This result is in contradiction with the literature (Reinhardt 1990) where a slight increase of ϵ_u with increasing strain rate is reported.

The rate sensitivity of the poisson's ratio ν was also investigated (Brühwiler 1987). A reduction of ν was determined as the compressive strain rate applied to the concrete cylinder was increased. At a compressive strain rate 1000 times faster than the quasi-static one, ν decreased by 30 % compared to the quasi-static ν value. Similar results were reported by Takeda & Tachikawa (1971).

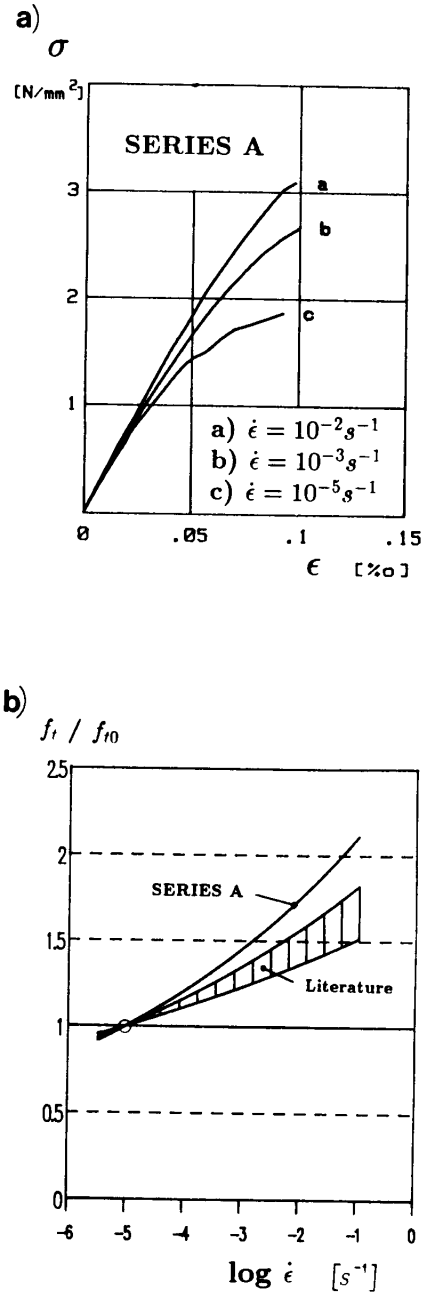

Figure 7. Results of direct tension tests: (a) stress against strain mean curves ($\epsilon = 1\ ‰ = 10^{-3}$), and (b) tensile strength as influenced by the strain rate.

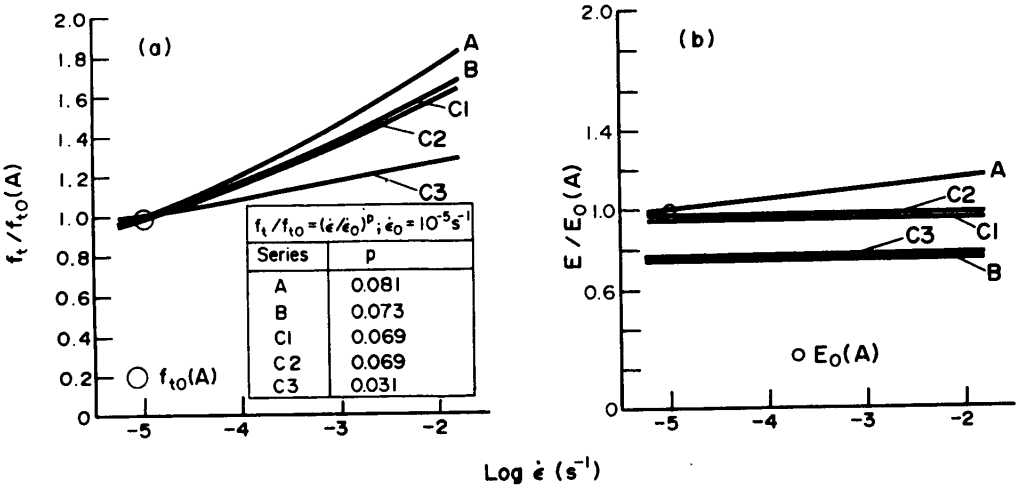

Figure 8. Effect of compressive pre-loading and high strain rates on: (a) tensile strength, and (b) modulus of elasticity. (All curves are normalized with respect to the quasi-static values $f_{t0}(A)$ and $E_0(A)$ of the concrete which was not pre-loaded, series A.)

4.42 Tensile tests after pre-loading (Series B, C1, C2, C3):

The results of direct tension tests (series A) are compared to those of tensile tests after initially applied compressive loading (series: B, C1, C2, C3).

- Irrespective of pre-loading, higher strain rates yielded higher tensile strength values (Figure 8a). At quasi-static strain rates, the tensile strength was not affected by pre-loading the concrete. This means that only the rate sensitivity, that is, the exponent p in Eq. 3, was reduced by compressive pre-loading.
- The effect of compressive pre-loading on the tensile strength in series B, C1 and C2 was relatively small. One compressive cycle to a relatively high strain (series B) resulted in about the same reduction of rate sensitivity of f_t as cyclic compressive pre-loading (series C1 and C2) at a strain level which corresponds to maximum computed compressive stresses occurring in dams under seismic conditions.
- Comparison between series B and C3 shows that a high strain level with cyclic loading led to a more significant reduction of the rate sensitivity. Reduction of rate sensitivity was the result of compressive cycles. Hence, the exponent p is dependent on the dissipated energy as the parameter to quantify the pre-loading rather than on the compressive strain level (Figure 12a) .
- However, variation in the number of cycles from 10 cycles (series C2) to 30 cycles (series C1) did not influence the tensile strength. Thus, the first few compressive cycles caused the reduction in tensile strength.
- Except for the mass concrete which was not pre-loaded, no rate sensitivity for the Young's modulus of pre-loaded concrete could be detected (Figure 8b). The higher the strain level of the compressive pre-loading, the greater was the reduction of E with respect to concrete which was not pre-loaded (Figure 12a). A significant reduction of the quasi-static Young's modulus as a result of compressive pre-loading was also reported by Hordijk & Reinhardt (1989).

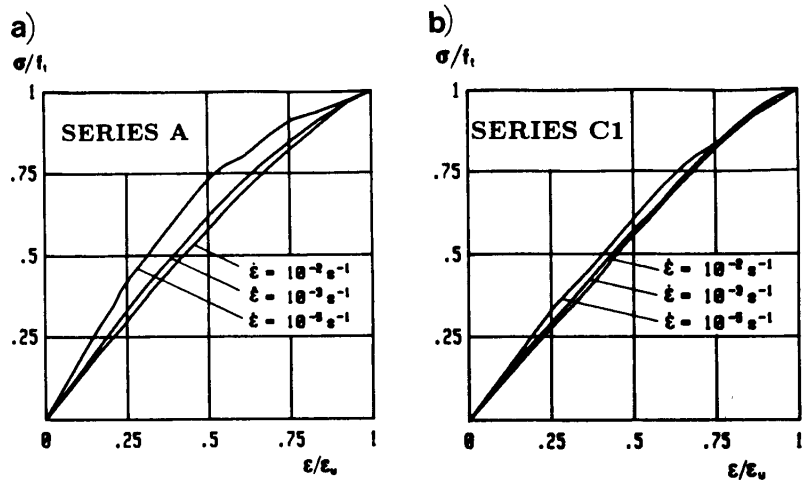

Figure 9. Normalized stress against strain curves of (a) direct tension tests, and (b) tests with pre-loading.

- No rate sensitivity could be observed for the ultimate strain ϵ_u, regardless of pre-loading. The ultimate strain increased with growing intensity of compressive pre-loading. Likewise, it increased with decreasing Young's modulus, and the energy stored in the specimen at tensile strength was the same irrespective of the pre-loading.

- The shape of the stress against strain diagrams can best be compared in the normalized presentation (Figure 9). The curvature of the normalized curves was smaller at high strain rate. That means that in both with and without pre-loading, the nonlinearity was less significant at high strain rates. Pre-loading led to an additional reduction of the nonlinearity of the normalized stress against strain curve.

4.5 Results from wedge splitting tests

4.51 Effect of deformation rate

The splitting force F_s against COD mean curves obtained for each COD rate are shown in Figure 10a. The relationship between the deformation rate and evaluated fracture properties is also expressed by a power law and plotted in Figure 11:

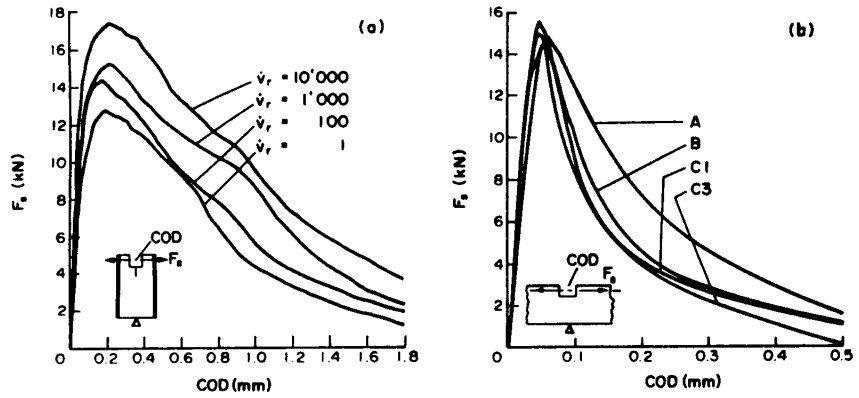

Figure 10. Splitting force against crack opening displacment curves (a) at four different defromation rates ($\dot{v}_r$ = 1; quasi-static deformation rate), and (b) as influenced by pre-loading at quasi-static deformation rate.

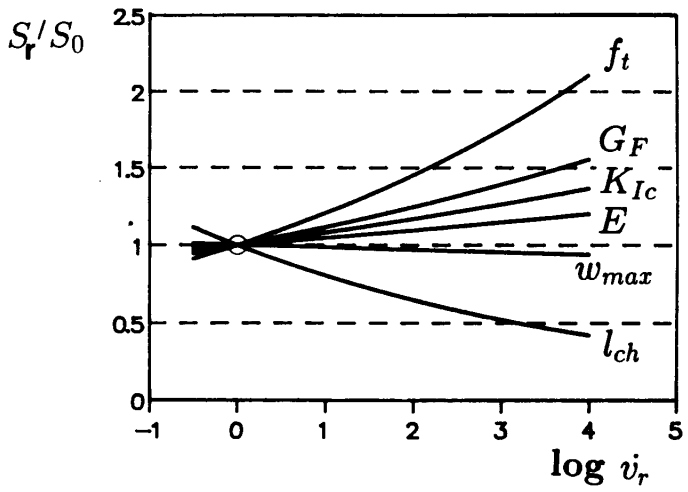

Figure 11. Effect of deformation rate on fracture properties of concrete which has not been pre-loaded.

- The F_s against COD curves at different deformation rates have similar shapes (Figure 10a). Higher deformation rates yielded higher G_F values. The following power law was determined for the rate sensitivity of G_F:

$$G_F = G_{F,0} \cdot (\dot{v}_r)^{0.048} \tag{9}$$

where $\dot{v}_r$ is the ratio between actual and quasi-static deformation rate. The G_F value at $\dot{v}_r = 10^4$ was some 56 % higher than the quasi-static G_F value.

- G_F was less rate sensitive than the tensile strength f_t. An exponent $p = 0.048$ was determined for G_F as compared to $p = 0.081$ for f_t. The rate sensitivity of the characteristic length l_{ch} of mass concrete which has not been pre-loaded is obtained by considering the rate sensitivity of f_t (Eq. 7), E (Eq. 8) and G_F (Eq. 9) and Eq. 2:

$$l_{ch} = l_{ch,0} \cdot (\dot{v}_r)^{-0.094} \tag{10}$$

Since l_{ch} is a measure for the length of the fracture process zone, this result indicates a significant decrease of the process zone length at high deformation rates.

- The numerically evaluated bilinear softening diagrams indicated slightly decreased values for the maximum fictitious crack width w_{max} with increased deformation rate. The numerically evaluated tensile strength values were less rate sensitive ($p = 0.055$) than the results from the uniaxial tensile tests (Eq.7). The normalized softening diagrams according to Figure 6b, were all within a narrow band, and, thus independent of the investigated deformation rates. Since the shape of the softening diagram remains similar, it follows that the rate sensitivity of w_{max} depends on the rate sensitivity of both G_F and f_t according to Eq. 5:

$$w_{max} = w_{max,0} \cdot (\dot{v}_r)^{-0.007} \tag{11}$$

- The rate sensitivity of the fracture toughness K_{Ic} was estimated using the relationship between K_{Ic} and G_F from LEFM (Eq. 1), Eqs 8 and 9:

$$K_{Ic} = K_{Ic,0} \cdot (\dot{v}_r)^{0.034} \tag{12}$$

K_{Ic} is less rate sensitive than G_F and f_t. At $\dot{v}_r = 10^4$, K_{Ic} is 38 % higher than the quasi-static fracture toughness.

According to LEFM concepts, K_{Ic} is a function of both the maximum force $F_{s,max}$ and the effective crack length a_{eff}. As l_{ch}, and thus the length of the FPZ, decreases with increasing deformation rate, the length of a_{eff} decreases also at high deformation rates. This is opposed to classical LEFM, where the crack length is set equal to the notch length in the specimen, and K_{Ic} is proportional to $F_{s,max}$.

- Higher deformation rates required higher maximum splitting forces $F_{s,max}$. According to the linear elastic strength of materials approach, the nominal strength of the fracture section, σ_N, is directly related to the maximum splitting force $F_{s,max}$:

$$\sigma_N = k \cdot F_{s,max} \tag{13}$$

where k is a constant depending on the geometry of the structure (specimen) only. From Eq. 13 it follows that normalized $F_{s,max}$ values describe the variation of the nominal strength as a function of deformation rate. The following power law was determined:

$$\sigma_N = \sigma_{N,0} \cdot (\dot{v}_r)^{0.037} \tag{14}$$

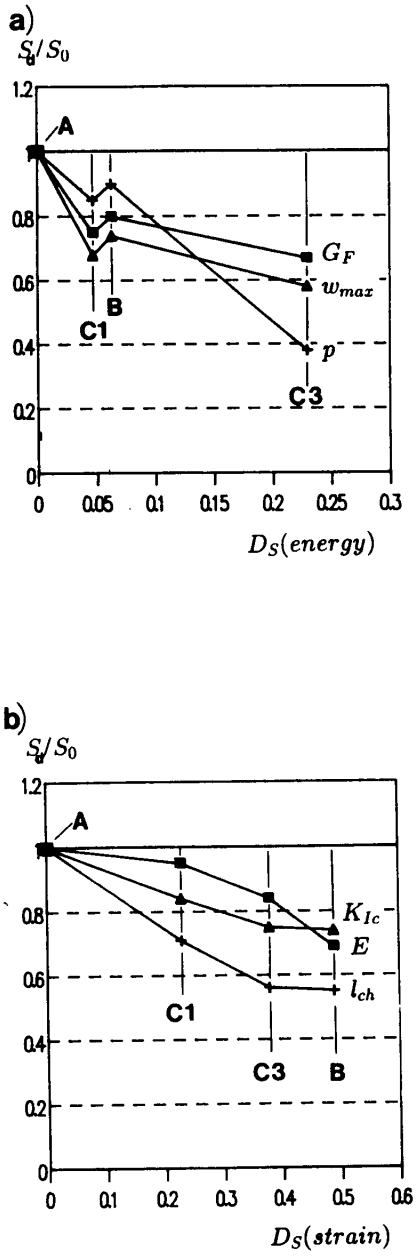

Figure 12. Effect of compressive pre-loading on quasi-static fracture properties. The 'intensity' of the pre-loading is expressed as (a) dissipated energy and (b) compressive strain level of the pre-loading.

4.52 Effect of compressive pre-loading at quasi-static deformation rate

The splitting force F_s against COD mean curves for each loading history are shown in Figure 10b. The effect of pre-loading on G_F, w_{max} and K_{Ic} is shown in Figure 12.

- The F_s against COD curves indicate steeper slopes of the descending branch (Figure 10b), and consequently, smaller G_F values caused by compressive pre-loading. This result is supported by Pons *et al.* (1988), but differs from Hordijk & Reinhardt (1989) who observed no decrease in G_F after pre-loading. This difference was explained by the fracture surface of their concrete which was characterized by an extensive amount of bond failures and complex crack paths. The fracture surfaces of the pre-loaded mass concrete in this study showed mainly aggregate failures.
- The maximum splitting force is not affected by pre-loading. This result coincides with findings from the uniaxial tensile tests and from the literature (Hordijk & Reinhardt 1989).
- Reduction of the specific fracture energy G_F turned out to be influenced more by compressive cycles (or dissipated energy) rather than by compressive strain level. Consequently, the 'intensity' of the compressive pre-loading was expressed in terms of dissipated energy (Figure 12a).
- The characteristic length l_{ch} and thus the FPZ length, decreased significantly as a result of pre-loading. For Series C3 with $E = 0.75 \cdot E_0$ and $G_F = 0.7 \cdot G_{F,0}$, the characteristic length is: $l_{ch} = 0.525 \cdot l_{ch,0}$ or almost 50 % shorter than for the concrete that had not been pre-loaded.
- The numerically evaluated bilinear softening diagrams revealed smaller values for the maximum fictitious crack width w_{max} (Figure 6a) with increasing intensity of the pre-loading. The numerically evaluated tensile strength was not influenced by pre-loading. The normalized softening diagrams were all within a narrow band and considered independent of pre-loading.
- According to Eq. 1, the fracture toughness K_{Ic} was found to be reduced with increasing intensity of pre-loading. For Series C3 with $E = 0.75 \cdot E_0$ and $G_F = 0.7 \cdot G_{F,0}$, the fracture toughness K_{Ic} is equal to $0.73 \cdot K_{Ic,0}$.

4.6 Description of damage and failure

The fracture surfaces of the specimens gave indications regarding failure and damage mechanisms having occurred as a result of compressive pre-loading and high deformation rates. In the following qualitative description of damage and failure mechanisms, concrete is considered as a composite material consisting of aggregates embedded in the cement matrix. Before concrete is loaded, microcracks exist in both the cement matrix and at the interface boundaries between matrix and aggregate inclusions, mainly because of cement hydration shrinkage.

On loading, high tensile stresses occur at the tip of these microcracks. As a result of compressive strain, tensile stresses occur at the interface boundaries between aggregates and the matrix, parallel to the compressive force (Figure 13a). The high stresses at the microcrack tips are relieved by propagation in the matrix and along the interface boundaries. The material is damaged. With increasing compressive pre-loading, more damage is accumulated in the material. On subsequent tensile loading (Figure 13b), the composite structure is separated along the weakened aggregate-matrix interface. The energy, and eventually the force, necessary to fracture the material, are reduced as a result of pre-loading, therefore leading to reduced fracture properties.

The influence of low and high deformation rates on failure of concrete is explained as follows. At a low deformation rate, there is enough time for microcrack propagation along the path of least resistance, that is, through weak aggregates and along the interface between the matrix and the aggregates. As a result, the fracture surface is characterized mainly by bond failures (Figure 14a). At high deformation rates, microcracks have to grow rapidly, and they propagate along shorter

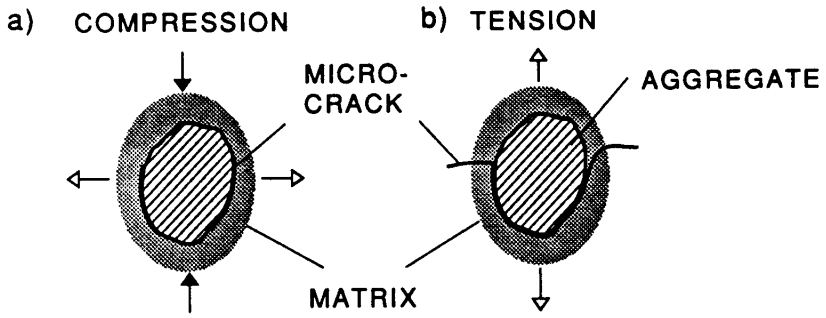

Figure 13. Schematic presentation of damaging of the bond between matrix and aggregate caused by (a) compressive pre-loading, and (b) subsequent tensile loading.

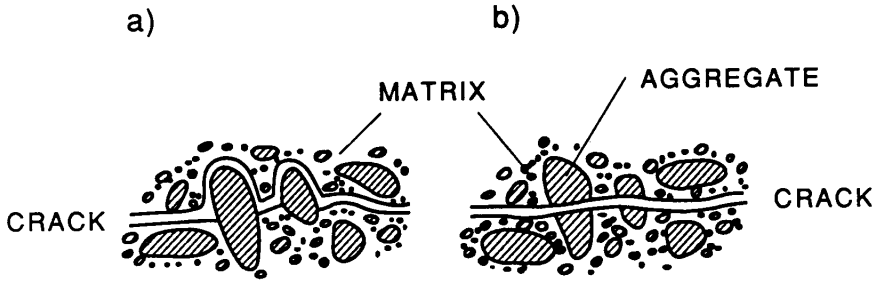

Figure 14. Schematic presentation of failure at (a) low and (b) high deformation rate.

paths through strong bonds and aggregates, resulting in more aggregate failures (Figure 14b). More energy and force is needed to fracture the material, therefore leading to higher values for the fracture properties at high deformation rates.

Subsequent to the uniaxial tensile experiments, the area of aggregate failure and bond failure of fracture surfaces was measured (Brühwiler 1987). Concrete which had not been pre-loaded showed an increase in the total area of broken aggregates with higher rates. Under the influence of compressive pre-loading, however, the area of aggregate failure was the same for all deformation rates tested. These results confirm the above qualitative description of damage and failure of concrete. Further experimental and theoretical studies are needed to fully understand damaging effects in concrete caused by mechanical loading.

5 Application of the test results

Based on the results of the present experiments under simulated seismic action, material models describing the tensile behaviour including fracture of mass concrete may be developed. Such models are needed for the modelling of crack formation in concrete dams subjected to seismic action. A procedure for the development of material laws is proposed:

- The tensile behaviour of concrete is subdivided into the linear elastic nonlinear stage preceding tensile strength for the description of continuous material under tensile stresses (Figure 1b), and a post-peak stage with tensile softening for the description of crack development and growth (Figure 1c).

- Simplified material laws describing linear or bilinear relationships are used in a first approximation as shown in Figure 2b.

- Normalized material laws are implemented in a computer code. Stresses and deformations are related to characteristic values such as the tensile strength, ultimate strain, maximum fictitious crack width and the ratio G_F/f_t:

  - Irrespective of the loading rate and pre-loading, one normalized stress against strain curve may be used (Figure 9).

  - According to the present results, the normalized bilinear softening law is independent of deformation rate and pre-loading. For mass concrete, typical values for the normalized bilinear softening parameters are: $\frac{s_1}{f_t} = 0.4$, $C_1 = 0.8$ and $C_2 = 3$ (Brühwiler 1988, see Figure 6).

- Absolute values S of fracture properties for the structural analysis are computed using the normalized material laws, the quasi-static properties S_0 of concrete which has not been pre-loaded, and normalized relationships describing effects of deformation rates and pre-loading. Such a transformation in its most general form is expressed as follows:

$$S = S_0 \cdot (1 - D_{S_1}) \cdot (\dot{v}_r)^{p \cdot (1 - D_{S_2})} \tag{15}$$

  According to the present test results, the relationship between fracture properties and deformation rate is described by a power law. The exponent p as well as the quasi-static fracture property S_0 may be influenced by pre-loading. Expressions for damage coefficients D_{S_i} can be developed on the basis of the results shown in Figure 12.

- A comprehensive sensitivity study is required to sort out fracture parameters sensitive to seismic action which do not affect the overall structural behaviour in a significant way and hence, may be neglected in order to simplify matters. This study should be conducted keeping in mind that numerical simulation of dams under seismic action is a very complex analysis including other aspects than modelling of crack formation.

In view of a general applicability of material laws in seismic analysis, various aspects must receive due attention. For upstream cracks, water eventually entering into an opening crack must be modelled realistically. Unloading/reloading during crack formation/propagation as well as variation of deformation rates occur during an earthquake. Also, multiaxial fracture properties as influenced by seismic action must be known especially for the analysis of arch dams. However, experimental studies dealing with all these aspects are very scarce.

Conclusion

1. The effects of both deformation rates and loading histories on fracture properties must be considered in the seismic analysis of a dam.
2. Fracture properties are generally influenced by rate effects and increase with increased deformation rate. The tensile strength and the specific fracture energy show a high rate sensitivity.
3. Compressive pre-loading generally leads to a material damage accompanied by a reduction of fracture properties. The specific fracture energy and the Young's modulus are most affected by pre-loading.
4. The effect of deformation rates and pre-loading is best presented in a normalized presentation where all values are related to the quasi-static fracture properties of unpre-loaded concrete. The normalized representation can serve for the elaboration of material models for tensile behaviour including crack formation in concrete dams under seismic action.
5. Tensile softening of mass concrete is more significant than softening of structural concrete. This is explained by the size and properties of the aggregates used for the construction of dams. The fracture process zone in dams may be large, and fracture energy models which account for the presence of the FPZ, should be applied for dam structures like arch dams, buttress dams and the crest section of gravity dams.

Acknowledgements

This research was performed under the auspices of Dr R. Biedermann, head of the Swiss Federal Direction of Water Economy, and Prof. Dr F.H. Wittmann at the Swiss Federal Institute of Technology (ETH). The writer appreciates their support in the publishing of this paper. In addition, thanks are due to Mr A. Helbling for his help in performing the uniaxial tensile tests and Mr H.L. Boggs for his thorough review of the paper.

Bibliography

M.L. AYARI AND V.E. SAOUMA, "A fracture-mechanics based seismic analysis of concrete gravity dams using discrete cracks", *Engineering Fracture Mechanics*, Vol. 35, No 1/2/3, pp. 587-598; 1990.

M.L. AYARI AND V.E. SAOUMA, "Static and dynamic contact/impact problems using fictitious forces", *International Journal of Numerical Methods in Engineering*, (submitted for publication); 1989.

Z.P. BAŽANT AND L. CEDOLIN, "Blunt crack propagation in finite element analysis", *Journal of the Engineering Mechanics Division*, ASCE Vol. 105, pp. 297–315; 1979.

Z.P. BAŽANT AND B.H. OH, "Crack band theory for fracture of concrete", *Materials & Structures*, Vol. 16, No 93, pp. 155-177; 1983.

E. BRÜHWILER, "Fracture mechanics of mass concrete subjected to quasi-static and seismic loading conditions", *Doctoral Thesis No 739*, Swiss Federal Institute of Technology, Lausanne; 1988 (in German).

E. BRÜHWILER, "Experiments on the influence of compressive pre-loading on the behaviour of mass concrete in tension at high strain rates", *Test Report*, Laboratory for Building Materials, Swiss Federal Institute of Technology, Lausanne; 1987 (in German).
E. BRÜHWILER AND F.H. WITTMANN, "The wedge splitting test, a method of performing stable fracture mechanics tests", *Engineering Fracture Mechanics*, Vol. 35, No 1/2/3, pp. 117-126; 1990.
E. BRÜHWILER, J.J. BROZ AND V.E. SAOUMA, "Fracture properties of dam concrete. Part III: Model assessment", *Journal of Engineering Materials*, ASCE (submitted for publication); 1989.
J. CHAPUIS, B. REBORA AND T. ZIMMERMANN, "Numerical approach of crack propagation analysis in gravity dams during earthquakes", *Proceedings*, Fifteenth ICOLD Congress, Q.57, R.26, Lausanne, pp. 451-474; 1985.
M. CURBACH, "Strength increase of concrete at high loading rates", *Doctoral Thesis*, Institute for Concrete Structures and Building Materials, Technical University Karlsruhe, Germany; 1987 (in German).
P. DROZ, "Numerical modelling of the nonlinear behaviour of massive unreinforced concrete structures", *Doctoral Thesis No 682*, Swiss Federal Institute of Technology, Lausanne; 1987 (in French).
L. ELFGREN [EDITOR], "Fracture Mechanics of Concrete Structures - From Theory to Applications", *Report RILEM TC 90-FMA*, Chapman & Hall, London; 1989.
G. FELTRIN, D. WEPF, AND H. BACHMANN, "Seismic cracking of concrete gravity dams", *DGEB Publication 4*, German Society for Earthquake Engineering and Structural Dynamics, Hannover; 1990.
GALILEO G., "Two new sciences", *cited in 'History of Strength of Materials'*, by S.P. Timoshenko, Dover Publications Inc., New York; 1983.
A. HILLERBORG, "Analysis of one single crack", *'Fracture Mechanics of Concrete'*, edited by F.H. Wittmann, Elsevier, Amsterdam, pp. 223-249; 1983.
A. HILLERBORG, M. MODÉER AND P.E. PETERSSON, "Analysis of crack formation and crack growth in concrete by means of fracture mechanics and finite elements", *Cement and Concrete Research*, Vol. 6, pp. 773-782; 1976.
D.A. HORDIJK, H.W. REINHARDT, "Influence of load history on mode I fracture of concrete", *Proceedings*, Fracture Toughness and Fracture Energy - Test Methods for Concrete and Rock edited by H. Mihashi et al, Balkema, Rotterdam, pp. 35-46; 1989.
G.R. IRWIN, "Analysis of stress and strain near the end of crack traversing plate", *Journal of Applied Mechanics*, 1957.
M. LORRAIN AND K.E. LOLAND, "Damage theory applied to concrete", *'Fracture Mechanics of Concrete'*, edited by F.H. Wittmann, Elsevier, Amsterdam, pp. 341-369; 1986.
H. MIHASHI AND F.H. WITTMANN, "Stochastic approach to study the influence of rate of loading on strength of concrete", *HERON (The Netherlands)*, No 25: 1980.
S. MINDESS AND S.P. SHAH [EDITORS], "Cement-based composites: strain rate effects of fracture", *MRS Symposia-Proceedings*, No 64, Materials Research Society, Pittsburgh; 1986.
J. MAZARS, "Mechanical damage and fracture of concrete structures", *Proceedings ICF5: Advances in Fracture Research*, Cannes 1981, Pergamon Press, Vol. 4, pp. 1499-1506; 1981.
G. PONS, S.A. RAMODA AND J.C. MASO, "Influence of the loading history on fracture mechanics parameters of microconcrete: effects of low-frequency cyclic loading", *ACI Materials Journal*, September-October issue, pp. 341-346; 1988.
H.W. REINHARDT, "Loading rate, temperature and humidity effects", *Fracture Mechanics of Concrete - Test Methods*, Report, RILEM TC 89-FMT, Chapman & Hall, London; 1990.
H.W. REINHARDT, "Strain rate effects on the tensile strength of concrete as predicted by thermodynamic and fracture mechanics models", *'Cement-based composites: strain rate effects of fracture'*, edited by S. Mindess and S.P. Shah, MRS Symposia-Proceedings No 64, Materials Research Society, Pittsburgh; 1986.
P.E. ROELFSTRA AND F.H. WITTMANN, "Numerical method to link strain softening with failure of concrete", *'Fracture Toughness and Fracture Energy of Concrete'*, edited by F.H. Wittmann Elsevier, Amsterdam, pp. 163-175; 1986.

V.E. SAOUMA, E. BRÜHWILER AND H.L. BOGGS, "A review of fracture mechanics applied to concrete dams", *Dam Engineering*, Vol. 1, Issue 1, pp. 41-57; 1990.
V.E. SAOUMA, J.J. BROZ, E. BRÜHWILER AND H.L. BOGGS, "Fracture properties of dam concrete - Part I: Laboratory Experiments", *Journal of Engineering Materials*, ASCE, (submitted for publication); 1989.
J. TAKEDA AND H. TACHIKAWA, "Deformation and fracture of concrete subjected to dynamic loading", *Proceedings*, International Conference on Mechanical Behaviour of Concrete, pp. 267-277; 1971.

Dam Engineering

Subscription

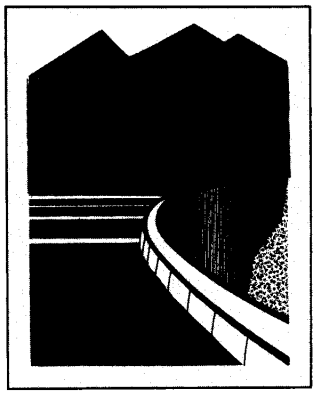

If you would like to subscribe to *Dam Engineering,* which is published quarterly, please write to the address below. The subscription rate is £110/US$175 per year (January to January). Cheques should be made payable to "Reed Business Publishing". Payment may also be made by credit card; please indicate the card type, the card number, the expiry date and the card holder's name. Alternatively, an invoice will be sent to you if you require one. Remember to include your full postal address. Please write to:

Dam Engineering
Room 922, Quadrant House
The Quadrant
Sutton, Surrey
SM2 5AS
UK